



The simulated multiple stars

prepared by: Frédéric Arenou
approved by: CU2
reference: GAIA-C2-SP-OPM-FA-054
issue: 1
revision: 0
date: 2010-01-28
status: Issued

Abstract

Binaries and multiple stars are a mandatory component in the simulation of the Milky Way. This note describes the properties of multiple stars as they have been implemented into the Universe Model part of the Gaia simulations from cycle 6 on.

Document History

Issue	Revision	Date	Author	Comment
1	0	2010-01-28	FA	Typos
D	0	2010-01-22	FA	First finished version after a one year delay...

Contents

1	Introduction	6
1.1	The recipe	6
2	Multiplicity fraction	7
2.1	Binary fraction	7
2.1.1	Main sequence stars	7
2.1.2	Giants	8
2.1.3	White dwarfs	8
2.2	Higher multiplicity fraction	10
3	Masses and orbital parameters	11
3.1	Mass-ratio	11
3.2	Semi-major axis	13
3.3	Eccentricity	13
3.4	Remaining orbital parameters	14
4	Close binary systems	15
5	Validation tests	15

6 Summary

16

Reference Documents

Abt, H.A., 2005, ApJ, 629, 507, ADS Link

Abt, H.A., 2006, ApJ, 651, 1151, ADS Link

Arenou, F., 2003, Java simulation of binaries, Tech. Rep. DMS-FA-03 (GAIA-C4-TN-OPM-FA-008-3), Observatoire de Paris / CNRS,
 URL <http://wwwhip.obspm.fr/gaia/dms/texts/DMS-FA-03.pdf>

Arenou, F., 2007, Recent simulations for the compression and on-board detection studies, Tech. Rep. PDH2-3120-TN-001.2 (GAIA-CA-TN-OPM-FA-046-2), Observatoire de Paris / CNRS,
 URL <http://wwwhip.obspm.fr/gaia/PDHS/restricted2/PDH2-3120-TN-001.pdf>

Barstow, M.A., Holberg, J.B., Fleming, T.A., et al., 1994, MNRAS, 270, 499, ADS Link

Bouy, H., Martín, E., Brandner, W., Bouvier, J., 2005, Astronomische Nachrichten, 326, 969, ADS Link

Burgasser, A.J., Kirkpatrick, J.D., Reid, I.N., et al., 2003, ApJ, 586, 512, ADS Link

Burgasser, A.J., Reid, I.N., Siegler, N., et al., 2007, Protostars and Planets V, 427–441, ADS Link

Close, L.M., Siegler, N., Freed, M., Biller, B., 2003, ApJ, 587, 407, ADS Link

Delfosse, X., Beuzit, J., Marchal, L., et al., 2004, In: R. W. Hilditch, H. Hensberge, & K. Pavlovski (ed.) Spectroscopically and Spatially Resolving the Components of the Close Binary Stars, vol. 318 of Astronomical Society of the Pacific Conference Series, 166–174, ADS Link

Duquennoy, A., Mayor, M., 1991, A&A, 248, 485, ADS Link

Eggenberger, A., Halbwachs, J.L., Udry, S., Mayor, M., 2004, In: Allen, C., Scarfe, C. (eds.) Revista Mexicana de Astronomia y Astrofisica Conference Series, vol. 21 of Revista Mexicana de Astronomia y Astrofisica Conference Series, 28–32, ADS Link

Eggleton, P.P., Tokovinin, A.A., 2008, MNRAS, 389, 869, ADS Link

Famaey, B., Jorissen, A., Luri, X., et al., 2005, A&A, 430, 165, ADS Link

Fleming, T.A., Snowden, S.L., Pfeffermann, E., Briel, U., Greiner, J., 1996, A&A, 316, 147, ADS Link

- Frankowski, A., Famaey, B., van Eck, S., et al., 2009, *A&A*, 498, 479, [ADS Link](#)
- Halbwachs, J.L., Mayor, M., Udry, S., Arenou, F., 2003, *Astronomy and Astrophysics*, 397, 159, [ADS Link](#)
- Holberg, J.B., Sion, E.M., Oswalt, T., et al., 2008, *AJ*, 135, 1225, [ADS Link](#)
- Kane, S.R., von Braun, K., 2008, *ApJ*, 689, 492, [ADS Link](#)
- Kobulnicky, H.A., Fryer, C.L., 2007, *Astrophysical Journal*, 670, 747, [ADS Link](#)
- Kouwenhoven, M.B.N., Brown, A.G.A., Zinnecker, H., Kaper, L., Portegies Zwart, S.F., 2005, *Astronomy and Astrophysics*, 430, 137, [ADS Link](#)
- Kouwenhoven, M.B.N., Brown, A.G.A., Portegies Zwart, S.F., Kaper, L., 2007, *Astronomy and Astrophysics*, 474, 77, [ADS Link](#)
- Kouwenhoven, M.B.N., Brown, A.G.A., Goodwin, S.P., Portegies Zwart, S.F., Kaper, L., 2008, *Astronomische Nachrichten*, 329, 984, [ADS Link](#)
- Lada, C.J., 2006, *ApJ*, 640, L63, [ADS Link](#)
- Mason, B.D., Gies, D.R., Hartkopf, W.I., et al., 1998, *Astronomical Journal*, 115, 821, [ADS Link](#)
- Mermilliod, J., Andersen, J., Latham, D.W., Mayor, M., 2007, *A&A*, 473, 829, [ADS Link](#)
- North, P., 2001, *Ecole de Goutelas #23*, CNRS, 22-26 May 2000, edited by D. Egret, J.-L. Halbwachs, and J.-M. Hameury. Publisher: Societe Francaise d'Astronomie et d'Astrophysique (SF2A), p. 67., 23, 67, [ADS Link](#)
- Pretorius, M.L., Knigge, C., O'Donoghue, D., et al., 2007, *MNRAS*, 382, 1279, [ADS Link](#)
- Reid, I.N., Cruz, K.L., Burgasser, A.J., Liu, M.C., 2008, *AJ*, 135, 580, [ADS Link](#)
- Sadowski, G., Siopis, C., Brandon, T., 2009a, [GESSS – Developer Manual](#), Tech. rep., Université Libre de Bruxelles, [DPAC svn link](#)
- Sadowski, G., Siopis, C., Brandon, T., 2009b, [Physical Models of Eclipsing Binary Systems](#), Tech. rep., Université Libre de Bruxelles, [DPAC svn link](#)
- Shatsky, N., Tokovinin, A., 2002, *Astronomy and Astrophysics*, 382, 92, [ADS Link](#)
- Söderhjelm, S., 2004, [Theoretical modelling of 'observational' double-star distribution functions.](#), Tech. Rep. DMS-SS-005, Lund Observatory,
URL <http://wwwhip.obspm.fr/gaia/dms/texts/DMS05b.pdf>
- Söderhjelm, S., 2007, *A&A*, 463, 683, [ADS Link](#)

- Sterzik, M.F., Durisen, R.H., 2004, In: Allen, C., Scarfe, C. (eds.) *Revista Mexicana de Astronomia y Astrofisica Conference Series*, vol. 21 of *Revista Mexicana de Astronomia y Astrofisica Conference Series*, 58–62, [ADS Link](#)
- Thies, I., Kroupa, P., 2007, *ApJ*, 671, 767, [ADS Link](#)
- Tingley, B., Sadowski, G., Siopis, C., 2009, In: *IAU Symposium*, vol. 253 of *IAU Symposium*, 402–403, [ADS Link](#)
- Tokovinin, A., 2008, In: *Multiple Stars Across the H-R Diagram*, *ESO Astrophysics Symposia*, 38–+, [ADS Link](#)
- Tokovinin, A., Thomas, S., Sterzik, M., Udry, S., 2008, In: S. Hubrig, M. Petr-Gotzens, & A. Tokovinin (ed.) *Multiple Stars Across the H-R Diagram*, 129–+, [ADS Link](#)
- Voyez, J., 2008, *Simulation d'étoiles binaires pour la préparation de la mission spatiale GAIA*, Tech. rep., Stage de Licence 3 Parcours Magistère, Université Paris Diderot

Acronym list

- BGM** Besançon Galaxy Model
- CV** cataclysmic variable
- EB** eclipsing binary
- MS** main sequence
- PMS** pre-main sequence
- SB** spectroscopic binaries
- VLM** very low mass
- WD** white dwarf
- WMC** Washington Multiplicity Catalog

1 Introduction

The Besançon Galaxy Model (BGM) model generates single stars only. Gaia will however notice or suffer from the effect of physical double and multiple stars in astrometry, photometry and spectroscopy, and it is highly desirable not only to simulate the orbital motion but also to reproduce as exactly as possible the various population properties of what is currently known about multiple stars. For this reason, simulations of binaries have been introduced in the Gaia simulator for long (Arenou, 2003).

In this first step, solar-type stars-like binaries were introduced only. Then simulations based on the Söderhjelm (2004) proposal were implemented; in summary, for each single star, a companion was created (or not) with some probability depending on the spectral type of the primary. The distribution of secondaries in separation and mass ratio was taken into account, the system could be visual, or astrometric binary with a main sequence or white dwarf companion. For visual systems, the initial luminosity was shared between components and the mass ratio followed from the magnitude difference, otherwise it was based on the luminosity of the primary.

Yet, the simulations were not satisfactory enough for several reasons: the single star fraction was severely underestimated towards low mass stars, multiple stars were not handled, and the resulting luminosity function was not consistent with the mass distribution. Accordingly, the generation of the secondaries or tertiary components has been completely changed at cycle 6 to achieve a more realistic simulation of the Galaxy.

1.1 The recipe

When a new star is drawn from the BGM, it may be changed with some probability into a system. Thanks to a software change in the BGM, it is now possible to draw a companion of a given mass on the HR diagram, coeval of the primary. The BGM has also been modified so that the single stars and primaries are chosen such that they follow the luminosity function (LF) of primaries in the solar neighborhood, not the LF of unresolved binaries, as was done before.

Using the primary mass, the mass of the companion is then obtained through a given statistical relation $q = M_2/M_1 = f(M_1)$, a process called a “primary-constrained pairing” in Kouwenhoven et al. (2008). A companion of this given mass is thus chosen in the HR diagram, with the same age as the primary. Beyond the preparation steps of this recipe, what matters really is the nature and quantities of the ingredients, all this being described below, with a large input from Voyez (2008).

2 Multiplicity fraction

The main observational effect of binaries come from their existing fraction relative to the total population. While a single number is often quoted (“more than half of stars are in binary systems”), things have changed since Duquennoy & Mayor (1991) (not all stars being considered of solar type for what concerns multiplicity!) and the available statistics have led Lada (2006) to provocatively argue that most stars are single (due to the low binarity rate of the most numerous star types).

2.1 Binary fraction

In what follows we call binary stars, or 2+, the systems having not two but at least two components, and more generally, following Tokovinin (2008), a_k denotes the fraction of systems containing at least k components.

2.1.1 Main sequence stars

Concerning main sequence (MS) solar type stars, the results from Duquennoy & Mayor (1991) have slowly been improved by studies using different range of periods. The statistics for the F7-K from Eggenberger et al. (2004) is 55.6% for $\log(P_{days}) < 6.31$. We adopt this value as the total fraction over all the period/separation range, which means that it is underestimated.

Towards the very low mass (VLM) part, the binary fraction is decreasing, about 28% for the M stars (Delfosse et al., 2004), 15% for the low mass M (Close et al., 2003), 12.5% from a complete sample in distance (Reid et al., 2008) of the ultracool L-dwarf population, and 9% for T brown dwarfs (Burgasser et al., 2003), probably underestimated (but not too much, see Figs 4a and 5) as it concerns separations $a \gtrsim 1$ AU and mass ratio $q \gtrsim 0.4$.

While the current scientific interest is often directed towards solar type down to very low mass stars, finding unbiased results for high-mass stars is still uneasy. For example, a $91 \pm 12\%$ binary fraction for $7 M_{\odot}$ stars may be found in Sterzik & Durisen (2004); however, this value is actually extrapolated, assuming a constant distribution in $\log a$ (commonly known as Öpik’s law), from the 0.20 ± 0.04 companion star fraction (mean number of companion per star) per decade of separation found by Shatsky & Tokovinin (2002) for B-type stars over a 0.3-6.4” separation range in Sco OB2.

Still in Sco OB2, Kouwenhoven et al. (2005) find a *detected* binary fraction $\approx 80\%$ for B0-B3 stars, $\approx 50\%$ for B4-B9 stars, $\approx 40\%$ for A-type stars. They demonstrate however that the decrease may be due to observational biases not taken into account. Later, correcting from incompleteness, Kouwenhoven et al. (2007) estimate that a binary fraction 85-100% for stars of spectral type B and 80-85% for those of spectral type A would better fit their data. Using the

lower limit, we assume 85% for earliest B stars ($20 M_{\odot}$) and 80% for earliest A stars ($3 M_{\odot}$). A similar result (a binary fraction from 0.8 to 1) is obtained in Cygnus OB2 by Kobulnicky & Fryer (2007).

The reason why we use the lower limit is that Mason et al. (1998) comparing the binarity in cluster/association, field or runaway O-type stars, suggests that almost all O-stars in clusters and associations have companions but that the binarity is much lower for field stars and still lower for the runaways. In the solar-type mass range, Halbwachs et al. (2003) comparing field and cluster stars show that the binary fraction for the latter is slightly larger though not significantly. All in all, we consider that this is perhaps not useful to adopt various proportions whether a star is in a cluster or not and the adopted fraction is actually a (not completely satisfactory, and still not well known however) compromise.

The function $f(M_1) = 83.88 \tanh(0.688M_1 + 0.079)$ fits rather well the binary fraction on the whole mass range (Fig. 1). The shape of this function was not chosen randomly but as roughly compatible (by eye) with the several classes of dynamical decay models from Sterzik & Durisen (2004) or random pairing of Thies & Kroupa (2007). However, the increase with primary mass over the short period solar type range which is assumed here deviates from the conclusion of Halbwachs et al. (2003) (finding no obvious proportion difference from F7 to late K) though perhaps not significantly.

2.1.2 Giants

The knowledge of the multiplicity fraction for giants has recently been improved, thanks to better statistical studies based on distance estimate from Hipparcos and CORAVEL radial velocity survey.

Improving the results initially given by Famaey et al. (2005), we use the binary fraction from Mermilliod et al. (2007) for the K giants and Frankowski et al. (2009) for the M giants. However, the fractions quoted here have been obtained for spectroscopic binaries (SB) (short periods) only and the completeness in period not really being indicated.

We have thus extrapolated these data for the whole period range to 60% and 25% respectively for K and M giants using a limit of primary mass $M_1 = 1.75$ for the limit between both. The period extrapolation is obviously based on some model (described in Sect. 3.2), such that there is a considerable uncertainty on the adopted numbers.

2.1.3 White dwarfs

At first sight, the probability for the companion of being a white dwarf (WD) could be based on the frequency of single white dwarfs in the BGM, which in turns depends on the age populations used in the model. In practice, it can be obtained from the ratio of the WD fraction over the star

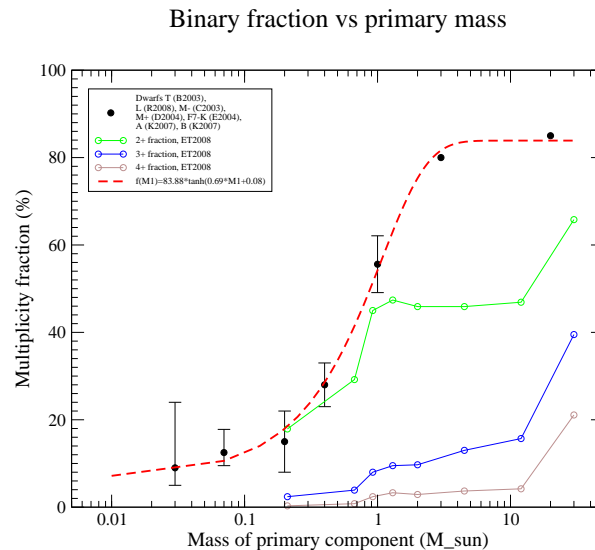


FIGURE 1: Binary fraction: the observed estimated fractions for different primary masses found in the literature (dots) and the fit proposed (dash red), and the 2+ fraction obtained in the ET2008 catalogue of multiplicity (green). From left to right, the points from the literature were obtained from Burgasser et al. (2003); Reid et al. (2008); Close et al. (2003); Delfosse et al. (2004); Eggenberger et al. (2004), and Kouwenhoven et al. (2007) for B and A stars. For comparison, the 3+ (blue) and the 4+ (orange) fractions from ET2008 are also indicated.

fraction (both transmitted by A. Robin, private communication) which does not actually vary much (between 8.8 and 9.1%).

The problem is that WD will enter in systems either as primary or as secondary, and an *ad hoc* trick has been needed as the resulting number of simulated couples with at least one WD was unfortunately not realistic enough (see below). Beside, the binary WD fraction cannot be a single number as it also depends on period and companion type.

Consequently, what has been done was to fine tune two numbers until satisfactory integration tests (see Sect. 5) are obtained. These tests are based on the fraction of systems with one WD obtained with ROSAT (Fleming et al., 1996) or Barstow et al. (1994), on the fraction of double degenerates (WD+WD) among systems with one WD or on Sirius-like binaries (A0-K7+WD) from Holberg et al. (2008), and the density of possible cataclysmic variable (CV)s per parsec cube (Pretorius et al., 2007) where a CV is defined here for operational purposes as a WD in a system with period < 0.6 day.

Currently, the assumption which allows satisfactory tests is that a secondary WD should be drawn with a 6.5% probability and that 90% of the CVs generated by default should be kept only.

2.2 Higher multiplicity fraction

Concerning now the simulation of higher level of multiplicity, the adopted fractions are mostly based on the extensive work by Tokovinin, and in particular from Eggleton & Tokovinin (2008) (ET2008). First, it can be noted that the a_k curves versus M_1 for the various k are rather similar (Fig. 1). Consequently, the fractions of 3+ may be obtained using the $a_2(M_1)$ curve, i.e. generating the binaries and then adding a tertiary component.

The frequency of triples among binaries is however strongly related to period, as can be seen in Tokovinin et al. (2008), p. 129: among solar type SBs with periods less than 30 days, $a_3/a_2 = 86\%$ of the systems with period below 5 days harbour a tertiary component versus 49% for those with a larger ($5 < P < 30$ days) inner period. To get the 3+ fraction for the rest of inner periods, we proceed as follow: we assume that the total fraction of triples a_3 for solar type stars is 8.4%, from Duquennoy & Mayor (1991), and from the assumed distribution of periods (Sect. 3.2) we thus use $a_3/a_2 = 11\%$ for $P > 30$ days.

Concerning now the 4+ systems, the relation between the multiplicity fractions mentioned above is shown Fig. 2. Although this ratio a_k/a_2 is obtained in ET2008 for a large $V < 6$ magnitude-limited sample, we adopt the $\exp^{-1.087(N-2)}$ fit to their probably more complete $V < 4$ sub-sample to generate the 4+, samples from the 3+ one, and the same fraction to get the 5+ from the 4+ number¹.

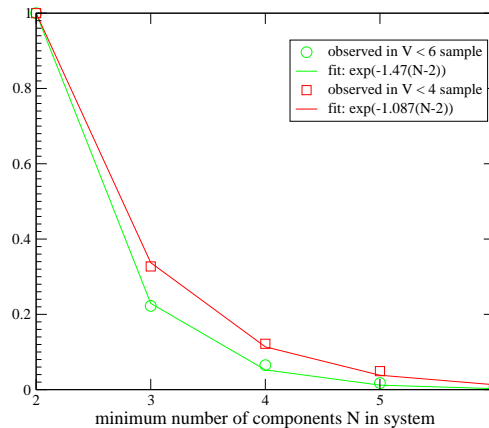


FIGURE 2: Observed probability to get systems with $N+$ component given that there are at least 2 components, from the ET2008 catalogue of multiplicity limited to magnitude 4 or 6.

Fig.3 shows the ET2008 results together with the adopted simulations. Only the simulation of the O type stars significantly deviates from ET2008, but this has already been discussed at sect. 2.1.1.

¹Actually, up to cycle 8, we have not simulated more than ternary components, as the simulated data are already complex enough (for the data reduction algorithms, not for the simulation!)

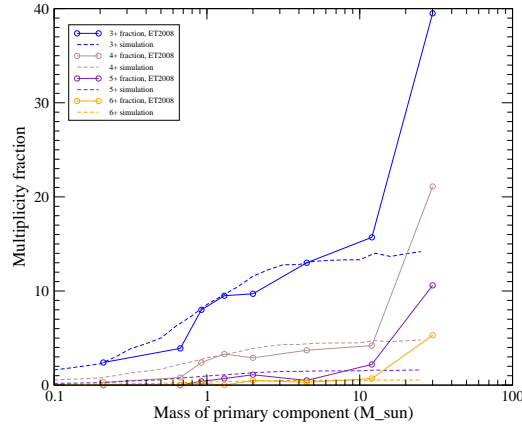


FIGURE 3: Observed (probably incomplete) multiplicity fractions versus primary mass from ET2008 and simulation (dashed lines) based on the binary simulation and period properties for triples, and an $\exp^{-1.09}$ relation for the higher multiplicity fractions.

3 Masses and orbital parameters

3.1 Mass-ratio

Once it is known that the star is actually a system, this star becomes the primary, and the secondary is generated through the choice of the mass-ratio. While, observationally, the primary of a system is conventionally the brighter, we use here the other convention, i.e. the primary is the one with the largest mass, and consequently the generated mass ratio is constrained to be $0 \leq q \leq 1$.

The mass ratio is estimated by rejection simulation using a probability density function linear by segment, and this, depending on the stellar type of the primary, and on the binary period, as illustrated Fig. 4. These simulations have been based on the works from (by increasing mass) Burgasser et al. (2007) for VLM, from (Delfosse et al., 2004, Fig. 4) for the M stars with period smaller or larger than 50 days, by (Halbwachs et al., 2003, Fig. 7) for the F7-K stars with period smaller or larger than 50 days, and by (Shatsky & Tokovinin, 2002, Fig. 9) for OB stars. The peak at $q = 1$ which historically has always been a matter of debate (as it may be produced e.g. by a photometric selection bias of twins) seems to be present at small periods, and it may even decrease with mass (Söderhjelm, 2007). Concerning this point, but also more generally, the simulated models should absolutely not be taken at face value as there is a considerable statistical uncertainty in the published results. Still, the simulated mass-ratios are better than a uniform distribution which would be adopted otherwise!

While the secondary is chosen based on the mass-ratio, it is however checked that the pairing is realistic, e.g. a pre-main sequence (PMS) star will be bound to another PMS, not a WD...

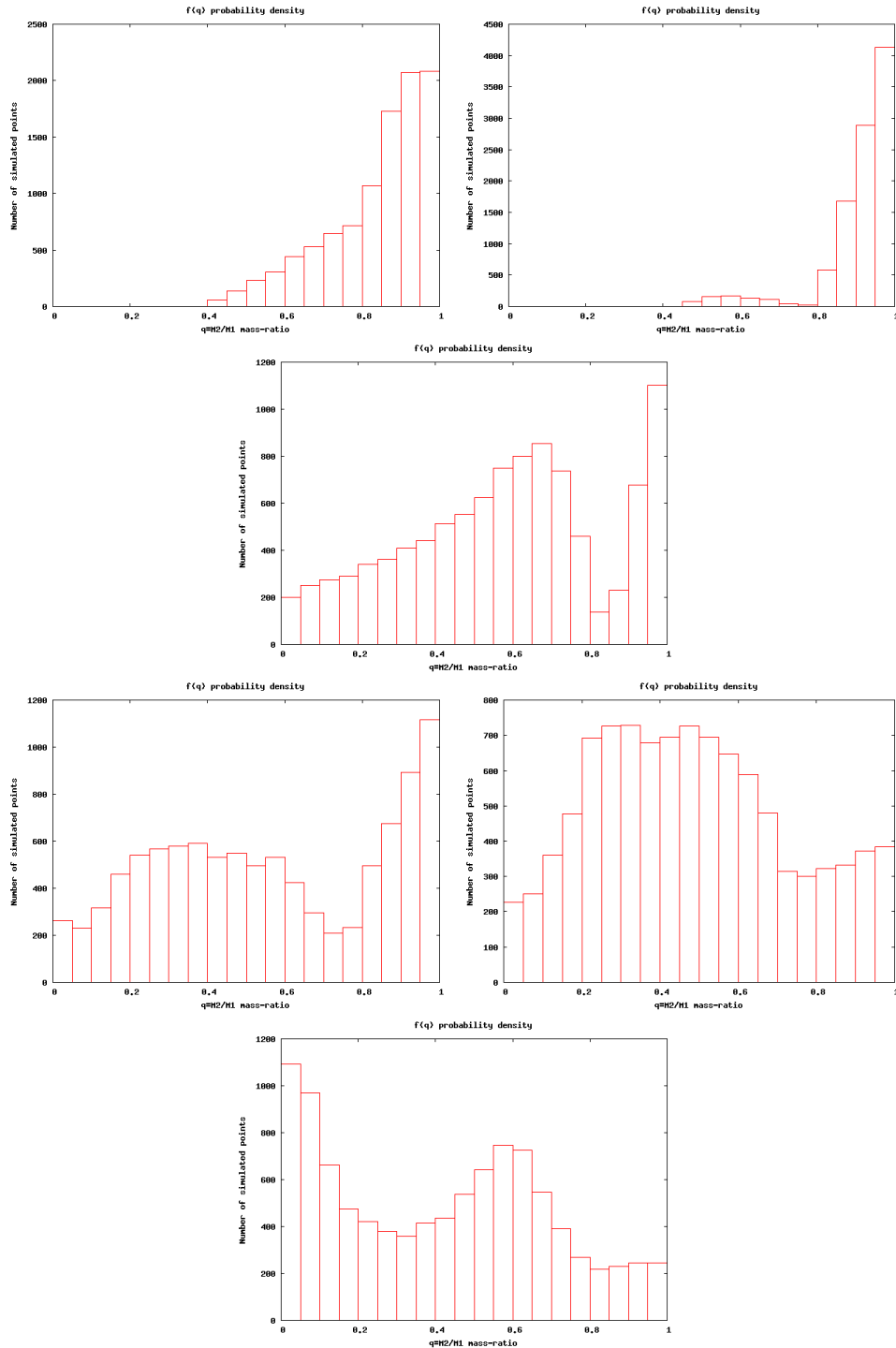


FIGURE 4: Simulated mass-ratio $q = M_2/M_1$ for (top to bottom): (a) very-low mass stars, (b) M stars with period $P < 50$ days or (c) $P > 50$ days, (d) solar type stars with $P < 50$ days, (e) solar type with $P > 50$ days, and (f) OB stars. See text for bibliographical references.

3.2 Semi-major axis

Beside their masses, the effect of binaries on astrometry, spectroscopy or photometry is mostly related to their period, or alternatively through the Kepler third law, to their separations.

For the distribution of semi-major axis a (A.U.), the classical Duquennoy & Mayor (1991) distribution for solar type stars, a Gaussian($\log a, 1.5, 1.5$), looks still very valuable and has been used here. However, M stars not only have a smaller binarity rate, but the separations are also smaller on the average. Separations are even smaller for ultracool binaries, Bouy et al. (2005) showing that most binaries have separations smaller to 20 A.U. We thus assume a Gaussian($\log a, 0.5, 0.5$) from Close et al. (2003). In between, it is estimated visually from Fig. 2 of Sterzik & Durisen (2004) that a Gaussian($\log a, 1, 1$) can be applied to the M stars (Fig. 5). On the other side of the H-R diagram, and lacking other statistics, we still assume the Duquennoy & Mayor (1991) separation properties for most massive stars.

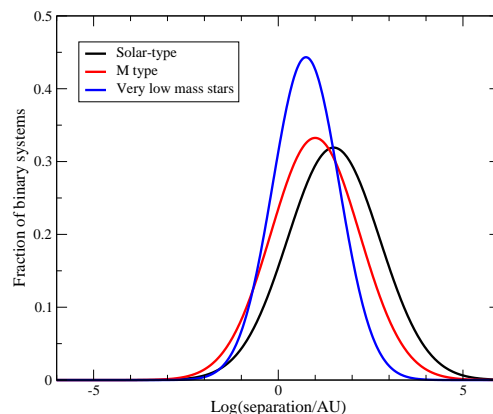


FIGURE 5: Distribution of the separations ($\log(\text{UA})$) as they are simulated. The broader curve on the right is the classical Duquesnoy & Mayor distribution, very low mass stars on the left and M stars chosen in between.

The Gaussian shape implies that very large separations are very rarely generated. The small separations are taken into account at Sect. 4. Once the separation is randomly generated that way, it is combined with the masses to obtain the orbital period.

3.3 Eccentricity

The orbital eccentricity is known from long to depend on period, at least because tidal effects lead to a circularisation of the orbit at small separations, cf. e.g. Abt (2005) and Abt (2006).

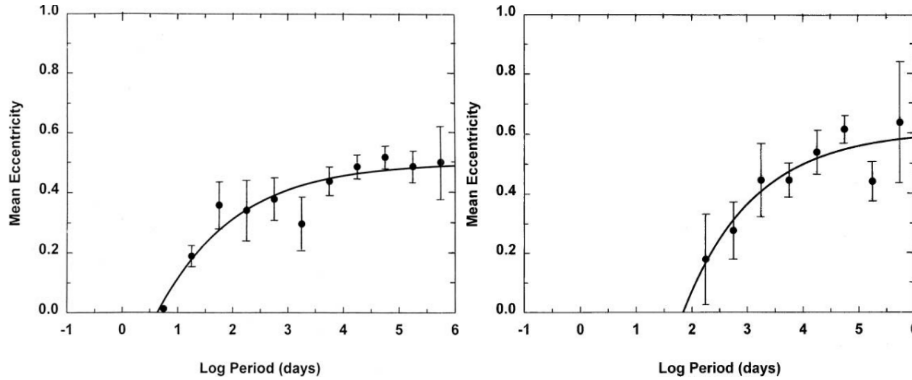


FIGURE 6: Average eccentricity as a function of orbital period for G dwarfs (left) and A-M giants or supergiants (right), from Abt (2006).

From Abt (2006), and as can be seen in Fig. 6, the average eccentricity can be written:

$$E[e] = a(b - \exp(-c \log P))$$

with the a, b, c coefficients given Table 1. Then, the eccentricity is simulated uniformly within the interval $[0, 2E[e]]$, possibly redrawing when larger than 1.

Type	Mass	a	b	c
B0-B9.5	> 3	0.587	0.935	0.449
A0-A5	> 2	0.646	0.819	0.982
A6-F0	> 1.6	0.646	0.857	0.440
F0-F9	> 1	0.708	0.816	0.686
G0-G9	> 0.8	0.792	0.631	0.723
K0-M5	> 0	1.153	0.383	1.522
(super)giants		2.600	0.235	0.787

TABLE 1: Coefficients for the average eccentricity as a function of period, foreach spectral type, and associated mass.

3.4 Remaining orbital parameters

The other orbital parameters are then drawn randomly. Random does not mean uniform, though. While the periastron date T is indeed chosen uniformly between 0 and the period P , the argument of the periastron ω_2 uniformly in $[0, 2\pi]$, the position angle of the node Ω uniformly in $[0, 2\pi]$, the inclination has to be random in $\cos i$, not in i .

4 Close binary systems

When a random separation is generated, a cutoff is obviously needed for small separations. For this purpose, we make use of a Roche model to avoid generating physically unrealistic systems.

The DU436 is the CU4 development unit which is in charge of handling the Gaia eclipsing binary (EB) data reduction. This has been, and still is, a very large human involvement to obtain a fully automated process of a complicated task (Tingley et al., 2009) within the DPAC development organisation. The code is based on, and tested against, the Wilson-Devinney and Nightfall codes. The physical models of eclipsing binary systems implemented in GESSS are described in Sadowski et al. (2009b) and the interface to the EB library is described in the GESSS Developer Manual (Sadowski et al., 2009a), to which the reader is referred. In order to solve an EB system, the DU436 algorithm, named GESSS, has a simulation step. As it was out of question to implement again this (many man-years) program, we have replaced our existing simplified implementation based on North (2001) and made use of GESSS from cycle 7 on.

Short period systems will undergo eclipses only when

$$(R_1 + R_2)(1 + e \cos(\pi/2 - \omega_2)) > (a_1 + a_2)(1 - e^2)|\cos i|$$

(cf. e.g. Kane & von Braun, 2008), where the radii R_j have the same physical unit as the semi-major axis a_j . We use GESSS not only for eclipsing systems, but also to check the likelihood of any generated small separation system². In a first step we change the inclination to force eclipses (before putting the correct value back) and call GESSS; then, if the generated system is physically unrealistic, it will be raised an exception (such as “eccentric over-contact”, “oversized surface”, or “fill factor too small” exceptions) and another separation is randomly drawn³.

5 Validation tests

Although we do not describe in this document how the simulations are implemented in practice, it should be noted that, beyond the basic JUnit unitary tests, integration tests have also been implemented. This is rendered mandatory by the statistical nature of the simulated data, and this is the projection into the observational domain, with a full generation of a large sample of stars suffering some selection biases, which may allow a meaningful validation of the simulation recipe through the comparison to the available data,

Table 5 shows the various tests which have been incorporated in the JUnit part of the code. The various selection biases of available published data are applied to generated samples, and the

²As the GESSS use can be very time consuming it is used only when a simplified Roche model shows that the separation is close enough

³this is attempted only once, two exceptions would stop the generation of a multiple system, returning the original single star instead

statistics on the simulated data are checked (within some error bar) to the comparison statistics. Beside, these tests are used as non-regression tests. The drawback is that the (twice a day) run of whole JUnit test on the Universe model is now very time and memory consuming as a very large size of sample has to be generated to get useful statistical error bars.

Test applied on the simulated data	Ref. value	Bibliography
Fractions of MS B-A, F-K, M+, M-, L or T binaries	cf. Fig. 1	cf. Fig. 1
Fraction of white dwarf being binaries	23%	ROSAT (1)
Fraction of WD+WD among WD	7/122	(2)
Fraction of Sirius-like among WD	8/122	(2)
Density of possible CVs per 1000 pc ³	0.011	(3)
Short period binary frequency of K giants	14.5%	(4) revised in (5)
Short period binary frequency of M giants	6.3%	(5)
Tycho+WDS, $m_A < 10.5$, $m_B < 11$, $0.2 < \rho < 1.5$ "	1.76%	(6)
F7-K SB, $d < 100$ pc, $P < 10$ yr, $q > 0.04$	13.5%	(7)
Long periods F7-K binaries, $q > 0.6$, $3.56 < \log(P) < 6.31$	9.3%	(8)
Total binary frequency, F7-K, $\log(P) < 6.31$	55.6%	(8)

TABLE 2: Statistics applied on the generated systems, in order to check if can be recovered the results by (1): Fleming et al. (1996), (2): Holberg et al. (2008), (3): Pretorius et al. (2007), (4): Mermilliod et al. (2007), (5): Frankowski et al. (2009), (6): Arenou (2007), (7): Halbwachs et al. (2003), (8): Eggenberger et al. (2004)

To illustrate the output generated by the simulations, a few graphs are shown below: the observed period-eccentricity diagram for all the generated pairs, Fig. 7, or the spectral type of the components, Fig. 8. How the apparent distribution shape of the mass-ratio and how the $q = 1$ peak may appear or not, depending on the sample selection, may be seen Fig. 9. Of course, the graph appearance depends both the multiple star model described above, and on the BGM properties.

6 Summary

With some probability, the binary proportion is given as a function of the type (mass) of the primary, and an (initially single) star given as input can give birth to a system. This system has the given star as primary, and a secondary which mass ratio is chosen at random, depending in a not-so-simple manner (it was taken for the available statistics) from the spectral type of the primary and on the binary period. As indicated above, the mass and age of secondary allow it to obtain physical parameters computed using the Hess diagram distribution in the Besançon model; with some probability this secondary can also be a white dwarf. Depending on the primary mass, the separation between components is chosen, and the period follows

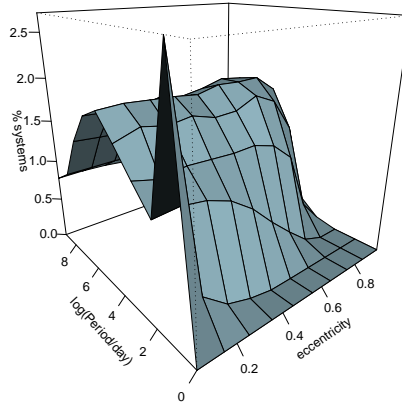


FIGURE 7: Observed period-eccentricity diagram.

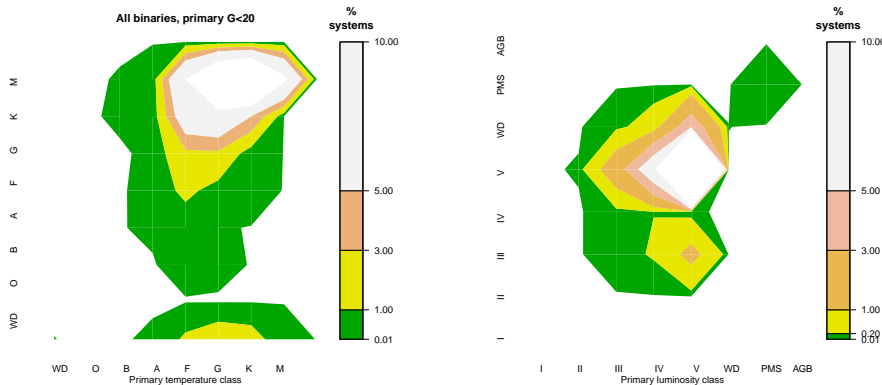


FIGURE 8: Proportion of pairs for the temperature classes (left) and luminosity classes (right): secondary versus primary component for all systems brighter than $G = 20$.

from Kepler third law, unrealistic small separations being avoided by the use of the external DU436 development. Drawing the random eccentricity depends on the primary type and period of the system. The other orbital parameters are chosen at random. Finally, ternary systems are also present, in accordance with latest fractions known from available observations. In this respect, the model of the Galaxy should now have achieved a large degree of realism. Some improvements are still to be done, e.g. to ensure that the variability due to close binaries is compatible with the observations.

Only the “static” part of the multiple star simulations has been described here. Beyond the Galactic properties of multiple stars, the astrometric, spectroscopic (radial velocity) and photometric (eclipses) effects of these objects on the transit observations have to be taken into account: in the course of the simulations of Gaia observations, the orbits are thus computed,

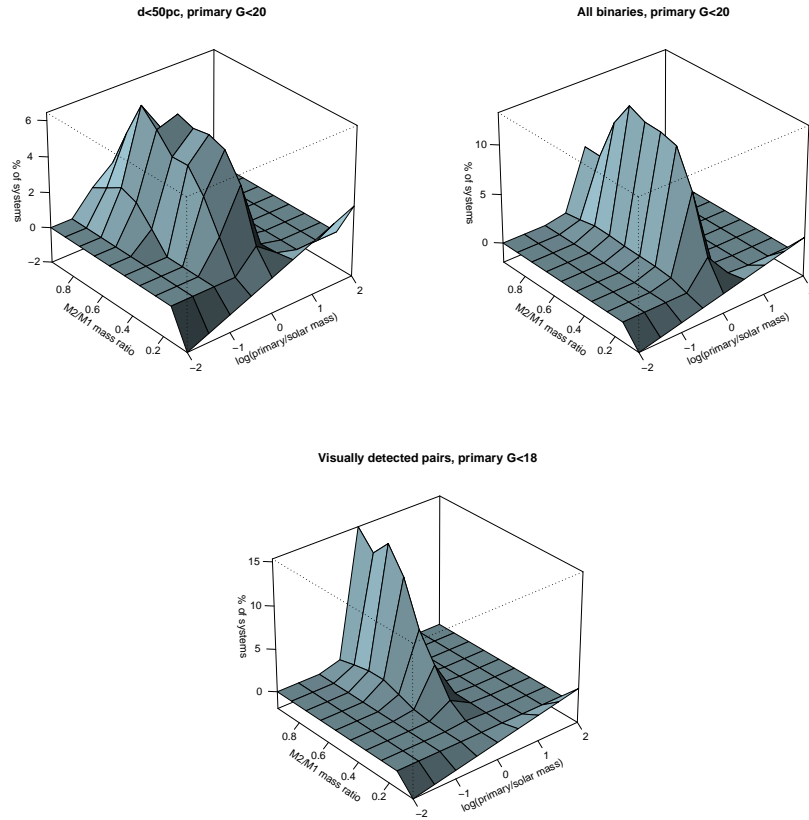


FIGURE 9: Mass ratio versus (log of) primary mass for a distance limited sample ($< 50\text{pc}$) or a $G < 20$ magnitude limited sample assuming that all components could be detected by astrometry, photometry or spectroscopy (far from true!), and a $G < 18$ sample where the two components can be “visually” resolved.

the positions/velocities/photometry of both components are modified accordingly. In particular, this means that the eclipses are computed, whatever the state of the system, and this is done by interfacing the software code developed by CU4 DU436. All this should be described in an update of Arenou (2003), a document which is now obsolete.